Journal of Zhejiang University-SCIENCE C (Computers & Electronics)
ISSN 1869-1951 (Print); ISSN 1869-196X (Online)
www.zju.edu.cn/jzus; www.springerlink.com
E-mail: jzus@zju.edu.cn

A robust optical/inertial data fusion system for motion tracking of the robot manipulator*

Jie CHEN[†1], Can-jun YANG[†‡1], Jens HOFSCHULTE[2], Wan-li JIANG[2], Cha ZHANG[1]

([1]*State Key Laboratory of Fluid Power Transmission and Control, Zhejiang University, Hangzhou 310027, China*)

([2]*ABB Corporate Research China, Shanghai 201319, China*)

[†]E-mail: chenjie.zju@gmail.com; ycj@zju.edu.cn

Received Oct. 23, 2013; Revision accepted Jan. 22, 2014; Crosschecked June 16, 2014

Abstract: We present an optical/inertial data fusion system for motion tracking of the robot manipulator, which is proved to be more robust and accurate than a normal optical tracking system (OTS). By data fusion with an inertial measurement unit (IMU), both robustness and accuracy of OTS are improved. The Kalman filter is used in data fusion. The error distribution of OTS provides an important reference on the estimation of measurement noise using the Kalman filter. With a proper setup of the system and an effective method of coordinate frame synchronization, the results of experiments show a significant improvement in terms of robustness and position accuracy.

Key words: Data fusion, Optical tracking, Inertial measurement unit, Kalman filter
doi:10.1631/jzus.C1300302 **Document code:** A **CLC number:** TP23

1 Introduction

Motion tracking of robot manipulators, which is needed for kinematic calibration or real-time motion control (Su *et al.*, 2009; Shirinzadeh *et al.*, 2010; Park *et al.*, 2012), requires high accuracy and robustness. The optical tracking system (OTS) using cameras or laser-assisted vision technology is one of the most common methods for motion tracking of robot manipulators. Advantages are high-accuracy position and orientation tracking ability, easy setup and good adaptability. It is more accurate than encoders using multiple links which will cause a cumulative error. Furthermore, by using markers, it is easy to set up and applicable for many cases. However, it also has some shortcomings. First of all, OTS with reflective markers always suffers from the marker-missing problem caused inevitably by disturbance and obstruction from other objects and uneven error distribution in the workspace due to the distortion of camera's lens and other configurations of OTS (Wiles *et al.*, 2004; Aristidou *et al.*, 2008). Thus, it is not robust enough for applications of industrial robots. Besides, the use of OTS, especially those with high performance, is always limited by the high cost. For example, the Leica absolute tracker AT901 (Leica Geosystems, Switzerland) costs about 100k USD, which is too expensive for many applications. Recently some low-cost OTSs have been launched in the market. They are generally used in applications that do not require high accuracy, such as human motion tracking. For example, the OTS used in our research costs about 10k USD, along with its software. These low-cost OTS have relatively low accuracy. Due to distortion of the cameras, the tracking accuracy in some areas of the workspace of OTS can be dramatically low. In this paper, a method for improving a low-cost OTS in terms of accuracy and robustness is developed using data fusion with an inertial measurement unit.

‡ Corresponding author

* Project supported by the National Natural Science Foundation of China (No. 51221004) and Sponsored Research between ABB Research Ltd. and Zhejiang University

2 Related work

Inertial measurement units (IMUs) are electronic devices that measure velocity, orientation, and gravitational forces using a combination of accelerometers and gyroscopes, sometimes also magnetometers. Owing to low cost, light weight, and quick response, IMUs have been widely used for navigation of vehicle/aircraft and human motion detection (Syed *et al.*, 2008; Dong *et al.*, 2010; Yun *et al.*, 2012). IMU has good short-term precision and high sampling rates, but it suffers from serious errors in long-term position and orientation estimates due to the drift and the algorithm of integration (Zhou and Hu, 2010). It has already been used to improve the performance of a Global Positioning System (GPS) based navigation system in terms of dynamic behavior, synchronization, and reliability (Sukkarieh *et al.*, 1999; Zhang *et al.*, 2005; Caron *et al.*, 2006).

Multi-sensor management is formally described as a system or a process that seeks to manage or coordinate the use of a suite of sensors or measurement devices in dynamic, uncertain environments, to improve the performance of data fusion and ultimately that of perception (Xiong and Svensson, 2002). It has become increasingly popular in industry and scientific research. There are several multi-sensor systems that combine OTS and IMU developed for surgical navigation (Claasen *et al.*, 2011; Ren *et al.*, 2012; Soroush *et al.*, 2012), user tracking in augmented reality (Foxlin *et al.*, 2004; Bleser and Stricker, 2009), and human motion detection (Tao and Hu, 2008; Zhang and Wu, 2011). By data fusion with IMU, the improvement of OTS includes three aspects, which are accuracy improvement in both position and orientation, sampling rate improvement, and reliability improvement by data compensation when markers in OTS are missing. Research aimed at some specific applications has proved that data fusion methods work well for orientation accuracy improvement and sampling rate improvement. However, the performance of OTS was not evaluated before data fusion in previous research, so the uneven error distribution of OTS was not considered. Furthermore, those approaches focused mainly on pose estimation and sampling rate improvement, and there are seldom descriptions or satisfactory results on position accuracy improvement and data compensation in position when markers are missing.

3 Performance evaluation of OTS

The Kalman filter operates recursively on streams of noisy input data to produce a statistically optimal estimate of the underlying system state. Thus, the determination of process noise covariance and measurement noise covariance is very important for the implementation of the Kalman filter. In our research, the data from OTS is treated as measurement of the true state. To obtain a more precise estimation of measurement noise covariance, a performance evaluation of OTS is needed. As the accuracy of OTS varies, the noise covariance of OTS in different areas of its workspace should be treated differently. Thus, during the performance evaluation, the workspace of OTS is divided into several areas and the error of each area is evaluated separately. The measurement noise covariance of OTS used in the Kalman filter is estimated due to the evaluation result of each area.

The OTS used in our research consists of six cameras, positioned as a circle (Fig. 1). A test case is designed to check the error distribution of OTS. A 300 mm×300 mm steel plate with 25 holes is designed for the test (Fig. 2). By placing the plate in different locations of the workspace, the position error of each area can be calculated by comparison with the real position of the markers. In each area, three samples are acquired at three different heights, which are 0.7, 1.0, and 1.3 m.

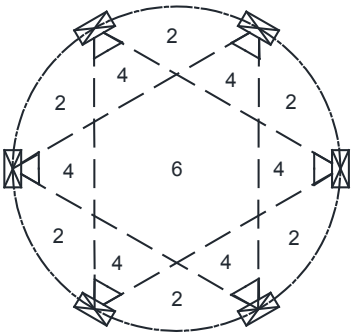

Fig. 1 Positioning of the six cameras

The diameter of the circle is 2.5 m, and the height of each camera is 1.8 m. The number in each area indicates the number of cameras that can cover the area

One result of the marker position detected by OTS is as shown in Fig. 3. After integration of all results in different areas of the workspace, we have the error distribution of OTS (Fig. 4). As we can see, the error in the edge of the workspace is larger than

that in the center. There are mainly two reasons for this uneven error distribution. First, the number of cameras by which the marker can be detected varies with the area in the workspace. As shown in Fig. 1, the center is in the visual field of all the six cameras, while the edges are covered with fewer cameras, which leads to a decrease of accuracy. Second, the visual field of each camera may still have some distortion, although they have already been calibrated. Thus, the measurement covariance of OTS using the Kalman filter should be treated differently in different areas.

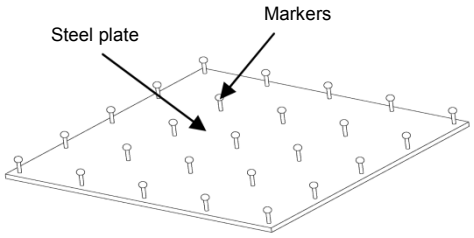

Fig. 2 A 300 mm×300 mm steel plate with 25 holes for marker placement

Markers are placed in these holes, whose position errors are less than 0.01 mm

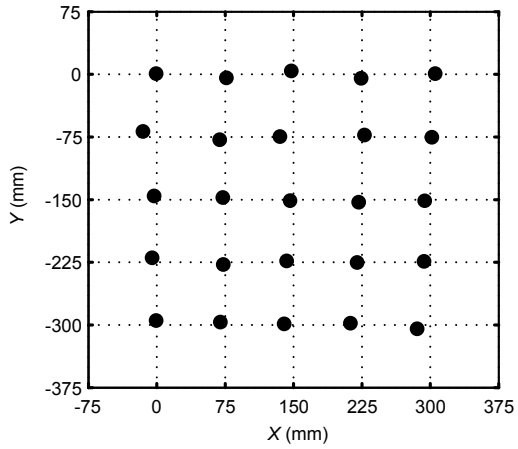

Fig. 3 Marker position detected by OTS

The position error of each marker is multiplied by a factor of 10. The position error of each marker is not even, and the average position error is 0.6339 mm

4 System configuration

The measurement system for the proposed method consists of an ABB IRB120 robot, an OTS for 6D tracking, and an IMU.

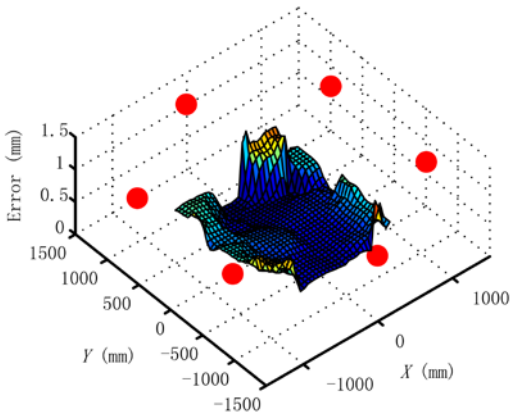

Fig. 4 Error distribution of OTS (● denotes the position of each camera)

4.1 Sensor system

The OTS used for this study consists of six V100:R2 cameras (NaturalPoint, Inc., USA) with its software Tracking Tools. Through the three reflective markers provided on the tool at the end of the robot, OTS is able to calculate both the position and orientation of the tool. The orientation of a tracking object is described in the form of quaternion in the tracking system. Hence, the pose of the tool calculated by OTS in the cameras' coordinate frame CF_{ots} is

$$_{(ots)}\boldsymbol{\varepsilon}_{p}=[x,y,z,q_x,q_y,q_z,q_w], \tag{1}$$

where (x, y, z) is the position and q_x, q_y, q_z, q_w are the quaternions which represent the orientation.

An MTi (Xsens Technologies B.V., The Netherlands) inertial measurement unit is used in our system (Fig. 5). It consists of a 3D MEMS acceleration sensor, a 3D MEMS gyroscope, and a 3D earth-magnetic field sensor. The IMU can provide the calibrated accelerations in three axes with gravity and the rates of turn in its body frame CF_{imu}. With a combination of the earth-magnetic field sensor, IMU is able to measure its orientation in the world coordinate system with an accuracy of 0.1°. Unfortunately, the pose estimated by IMU cannot be trusted in our case as the motor of our robot disturbs the magnetic field sensor. Thus, only the accelerations and the angular velocities are used in our study:

$$_{(imu)}\boldsymbol{\varepsilon}=[a_x,a_y,a_z,\omega_x,\omega_y,\omega_z], \tag{2}$$

where a_x, a_y, a_z are accelerations along the x-, y-, and

z-axis, respectively, and ω_x, ω_y, ω_z are angular velocities along the x-, y-, and z-axis, respectively.

The IMU's maximum sampling rate is 512 Hz. In our setup, we acquire data with a sampling rate of 100 Hz, which is the same as in the optical tracking system.

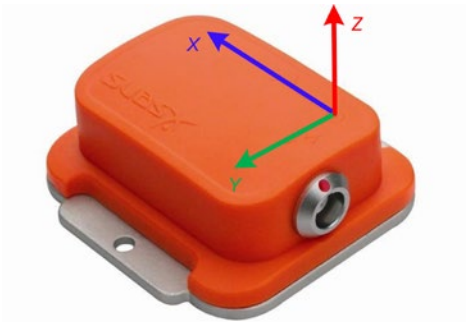

Fig. 5 Xsens MTi inertial measurement unit

4.2 System setup

The setup of the system is shown in Fig. 6. The six cameras of OTS are placed as a circle, and an industrial robot IRB120 (ABB) is placed at the center of OTS's workspace for the tests. The introduced IMU is equipped at the end effector (EE) of a robot along with three reflective markers. The robot allows high repeatability movements to verify the proposed method for position and orientation estimation. All the algorithms are developed using MATLAB, running in a sampling time less than 10 ms. After the setup of the system, we have to calibrate OTS first, including defining the coordinate frame of OTS.

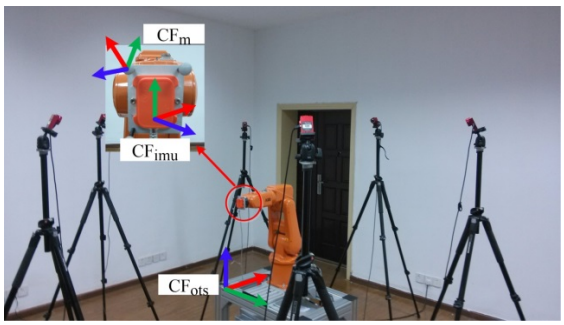

Fig. 6 System setup with OTS, a robot, and IMU

4.3 Synchronization of the coordinate frame

The data acquired from the introduced measurement sensors is given in different coordinate frames, i.e., the coordinate frame of OTS CF_{ots} and the coordinate frame of IMU CF_{imu}. The former is treated as the world's coordinate frame CF_{ots}. Although IMU can detect its own orientation in the world coordinate system, in our case it is disturbed greatly by the motor of the robot. Hence, another synchronization of coordinate frames from CF_{imu} to CF_{ots} is needed to combine the data using the fusion algorithm. This step is extremely important because it has a great influence on gravity compensation, which may lead to bad quality of data fusion with a small deviation.

The homogeneous transformation matrix of the three markers ${}^{ots}\boldsymbol{R}_{m}$ and the acceleration vector of IMU with respect to their own coordinate frames are provided directly by the two sensor systems. To combine these two coordinate frames, we have to find the homogeneous transformation matrix between the markers and the IMU ${}^{m}\boldsymbol{R}_{imu}$. It is a fixed homogeneous transformation matrix as the markers and the IMU are fixed on one frame. One method is just matching the axis of the two coordinate frames by estimation. However, a better method is calculating the exact homogeneous transformation matrix ${}^{m}\boldsymbol{R}_{imu}$. After it is calculated, we can transfer the data of IMU into cameras' coordinate system CF_{ots} in real time using the homogeneous transformation matrix ${}^{ots}\boldsymbol{R}_{imu}$:

$$ {}^{ots}\boldsymbol{R}_{imu} = {}^{ots}\boldsymbol{R}_{m}\,{}^{m}\boldsymbol{R}_{imu}\,. \tag{3} $$

A synchronization method using the direction of gravity is proposed. First of all, when placing the ground plane to set the coordinate frame of OTS, we can use the two bubble levels on the plane, whose resolution is 30′, to ensure that the y-axis of the world's coordinate frame CF_{imu} matches the vertical direction (Fig. 7). The IMU can also detect the vertical direction using the accelerometer. Thus, we can check the acceleration vector in the world's coordinate frame CF_{ots} in some specific conditions. We can calculate the exact homogeneous transformation matrix ${}^{m}\boldsymbol{R}_{imu}$ using the following equation:

$$ \mathbf{acc}_{ots} = {}^{ots}\boldsymbol{R}_{m}\,{}^{m}\boldsymbol{R}_{imu}\mathbf{acc}_{imu}\,. \tag{4} $$

As shown in Fig. 7, when the IMU's three axes are adjusted to match the vertical direction, we can write the acceleration matrix $\mathbf{acc}_{ots}$ in CF_{ots} directly:

$$ \mathbf{acc}_{ots} = [0 \quad g \quad 0]^{\mathrm{T}}, \tag{5} $$

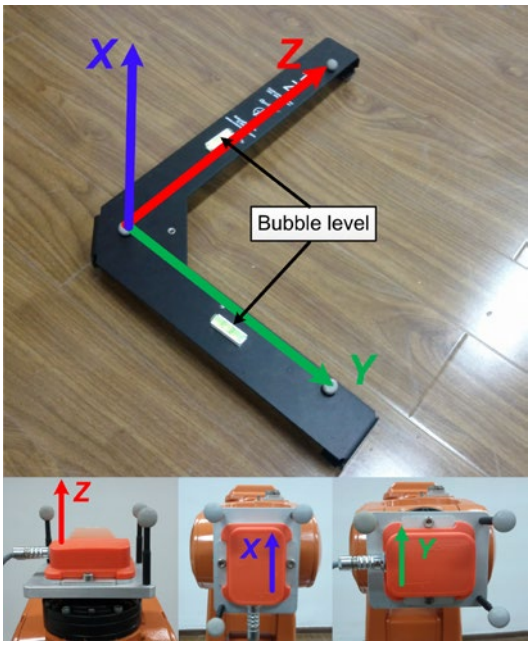

Fig. 7 Coordinate frames of OTS and IMU

where g represents the acceleration due to gravity. At the same time, we can check the acceleration matrix $\mathbf{acc}_{\mathrm{imu}}$ in the coordinate frame of IMU $\mathrm{CF}_{\mathrm{imu}}$ in the following three conditions:

$$(\mathbf{acc}_{\mathrm{imu}})_{x\mathrm{Up}}=\begin{bmatrix}g & 0 & 0\end{bmatrix}^{\mathrm{T}}, \tag{6}$$

$$(\mathbf{acc}_{\mathrm{imu}})_{y\mathrm{Up}}=\begin{bmatrix}0 & g & 0\end{bmatrix}^{\mathrm{T}}, \tag{7}$$

$$(\mathbf{acc}_{\mathrm{imu}})_{z\mathrm{Up}}=\begin{bmatrix}0 & 0 & g\end{bmatrix}^{\mathrm{T}}, \tag{8}$$

where $(\mathbf{acc}_{\mathrm{imu}})_{x\mathrm{Up}}$, $(\mathbf{acc}_{\mathrm{imu}})_{y\mathrm{Up}}$, and $(\mathbf{acc}_{\mathrm{imu}})_{z\mathrm{Up}}$ are the acceleration matrices measured by IMU in each condition.

Assume the homogeneous transformation matrix is

$${}^{\mathrm{m}}\boldsymbol{R}_{\mathrm{imu}}=\begin{bmatrix}r_{11} & r_{12} & r_{13}\\ r_{21} & r_{22} & r_{23}\\ r_{31} & r_{32} & r_{33}\end{bmatrix}. \tag{9}$$

We can calculate the homogeneous transformation matrix ${}^{\mathrm{m}}\boldsymbol{R}_{\mathrm{imu}}$ that maps the orientation of IMU $\mathrm{CF}_{\mathrm{imu}}$ to the orientation of markers CF_{m} by the following three equations:

$$\mathbf{acc}_{\mathrm{ots}}=({}^{\mathrm{ots}}\boldsymbol{R}_{\mathrm{m}})_{x\mathrm{Up}}\,{}^{\mathrm{m}}\boldsymbol{R}_{\mathrm{imu}}(\mathbf{acc}_{\mathrm{imu}})_{x\mathrm{Up}}, \tag{10}$$

$$\mathbf{acc}_{\mathrm{ots}}=({}^{\mathrm{ots}}\boldsymbol{R}_{\mathrm{m}})_{y\mathrm{Up}}\,{}^{\mathrm{m}}\boldsymbol{R}_{\mathrm{imu}}(\mathbf{acc}_{\mathrm{imu}})_{y\mathrm{Up}}, \tag{11}$$

$$\mathbf{acc}_{\mathrm{ots}}=({}^{\mathrm{ots}}\boldsymbol{R}_{\mathrm{m}})_{z\mathrm{Up}}\,{}^{\mathrm{m}}\boldsymbol{R}_{\mathrm{imu}}(\mathbf{acc}_{\mathrm{imu}})_{z\mathrm{Up}}, \tag{12}$$

where $({}^{\mathrm{ots}}\boldsymbol{R}_{\mathrm{m}})_{x\mathrm{Up}}$, $({}^{\mathrm{ots}}\boldsymbol{R}_{\mathrm{m}})_{y\mathrm{Up}}$, and $({}^{\mathrm{ots}}\boldsymbol{R}_{\mathrm{m}})_{z\mathrm{Up}}$ are provided by OTS in each condition.

5 Modeling

5.1 State models

To track the tool at the EE of the robot, both the position and orientation have to be estimated using the Kalman filter. The acceleration data $\boldsymbol{x}''_{\mathrm{imu}}$ provided by IMU contains gravitational acceleration g. Before it is used for estimation, a compensation for gravitation term g should be achieved:

$$\boldsymbol{x}''_{\mathrm{p}}(t)={}^{\mathrm{ots}}\boldsymbol{R}_{\mathrm{imu}}(t)\boldsymbol{x}''_{\mathrm{imu}}(t)-g, \tag{13}$$

where $\boldsymbol{x}_{\mathrm{p}}''$ is the acceleration vector of EE after gravity compensation, and ${}^{\mathrm{ots}}\boldsymbol{R}_{\mathrm{imu}}$ is the transform orientation matrix between IMU and OTS.

The angular velocities $\boldsymbol{x}'_{\mathrm{imu}}$ provided by IMU also need to be converted into the coordinate frame of OTS:

$$\boldsymbol{x}'_{\mathrm{o}}(t)={}^{\mathrm{ots}}\boldsymbol{R}_{\mathrm{imu}}(t)\boldsymbol{x}'_{\mathrm{imu}}(t), \tag{14}$$

where $\boldsymbol{x}_{\mathrm{o}}'$ is the angular velocity vector in the coordinate of OTS.

As a result, both object acceleration and orientation matrix should be considered for position estimation. Thus, a separate determination of the position and the orientation state space model is required. The classical differential equation for translation with acceleration and rotation with a constant angular velocity is

$$\boldsymbol{x}_{\mathrm{p}}=\boldsymbol{x}_{\mathrm{p}}^{\mathrm{ini}}+\boldsymbol{x}'_{\mathrm{p}}t+\boldsymbol{x}''_{\mathrm{p}}t^2/2, \tag{15}$$

$$\boldsymbol{x}_{\mathrm{o}}=\boldsymbol{x}_{\mathrm{o}}^{\mathrm{ini}}+\boldsymbol{x}'_{\mathrm{o}}t. \tag{16}$$

Thus, the state space vectors separated with position and orientation of the model are created as follows:

$$\begin{bmatrix}\boldsymbol{x}_{\mathrm{p}}(t)\\ \boldsymbol{x}'_{\mathrm{p}}(t)\\ \boldsymbol{x}''_{\mathrm{p}}(t)\end{bmatrix}, \tag{17}$$

$$\begin{bmatrix}\boldsymbol{x}_{\mathrm{o}}(t)\\ \boldsymbol{x}'_{\mathrm{o}}(t)\end{bmatrix}. \tag{18}$$

According to the classical differential equation for translation with acceleration and constant angular velocity, the discretized transition equations of the state space models concerning the position and orientation are

$$\begin{bmatrix} \boldsymbol{x}_{\mathrm{p}}(k) \\ \boldsymbol{x}'_{\mathrm{p}}(k) \\ \boldsymbol{x}''_{\mathrm{p}}(k) \end{bmatrix} = \begin{bmatrix} 1 & \Delta T & \Delta T^2/2 \\ 0 & 1 & \Delta T \\ 0 & 0 & 1 \end{bmatrix} \begin{bmatrix} \boldsymbol{x}_{\mathrm{p}}(k-1) \\ \boldsymbol{x}'_{\mathrm{p}}(k-1) \\ \boldsymbol{x}''_{\mathrm{p}}(k-1) \end{bmatrix}, \quad (19)$$

$$\begin{bmatrix} \boldsymbol{x}_{\mathrm{o}}(k) \\ \boldsymbol{x}'_{\mathrm{o}}(k) \end{bmatrix} = \begin{bmatrix} 1 & \Delta T \\ 0 & 1 \end{bmatrix} \begin{bmatrix} \boldsymbol{x}_{\mathrm{o}}(k-1) \\ \boldsymbol{x}'_{\mathrm{o}}(k-1) \end{bmatrix}, \quad (20)$$

where ΔT is the sampling time of the discretization.

5.2 Measurement models

According to the data provided by IMU and OTS, the equations for the position and orientation measurement models are

$$\begin{bmatrix} \boldsymbol{x}_{\mathrm{p}}(k) \\ \boldsymbol{x}'_{\mathrm{p}}(k) \\ \boldsymbol{x}''_{\mathrm{p}}(k) \end{bmatrix} = \begin{bmatrix} 1 & 0 \\ 1/\Delta T & 0 \\ 0 & 1 \end{bmatrix} \begin{bmatrix} \boldsymbol{x}_{\mathrm{p}}(k) \\ \boldsymbol{x}''_{\mathrm{p}}(k) \end{bmatrix} - \begin{bmatrix} 0 & 0 \\ 1/\Delta T & 0 \\ 0 & 0 \end{bmatrix} \begin{bmatrix} \boldsymbol{x}_{\mathrm{p}}(k-1) \\ \boldsymbol{x}''_{\mathrm{p}}(k-1) \end{bmatrix}, \quad (21)$$

$$\begin{bmatrix} \boldsymbol{x}_{\mathrm{o}}(k) \\ \boldsymbol{x}'_{\mathrm{o}}(k) \end{bmatrix} = \begin{bmatrix} 1 & 0 \\ 0 & 1 \end{bmatrix} \begin{bmatrix} \boldsymbol{x}_{\mathrm{o}}(k) \\ \boldsymbol{x}'_{\mathrm{o}}(k) \end{bmatrix}, \quad (22)$$

where position $\boldsymbol{x}_{\mathrm{p}}(k)$ and orientation $\boldsymbol{x}_{\mathrm{o}}(k)$ are measured by OTS, acceleration $\boldsymbol{x}_{\mathrm{p}}''(k)$ and angular velocity $\boldsymbol{x}_{\mathrm{p}}'(k)$ by IMU. Although $\boldsymbol{x}_{\mathrm{p}}'(k)$ can be estimated using the Kalman filter in the state model, the integration of acceleration will cause a great cumulative error. Thus, the measurement value of $\boldsymbol{x}_{\mathrm{p}}'(k)$ is also provided in the measurement model using the measurement value of the position, and the measurement noise covariance of velocity is estimated using the measurement noise covariance of the position.

6 Kalman filter

Kalman filters are widely used in sensor fusion applications. By data fusion with an IMU using a Kalman filter, we are expecting to improve the performance of the low-price OTS.

6.1 Implementation

Based on state models and measurement models, the following linear time-invariant stochastic difference equations, which represent the estimation and the measurement, are used to implement the Kalman filter:

$$x(k) = \Phi(T)x(k-1) + \omega(k), \quad (23)$$

$$y(k) = Cx(k) + \upsilon(k), \quad (24)$$

where $\Phi(T)$ is the state transition model, and C is the observation model. $\omega(k)$ and $\upsilon(k)$ account for process and measurement noises, respectively. They are assumed to be drawn from a zero mean multivariate normal distribution with covariances $Q(k)$ and $R(k)$.

6.2 Estimation of noise covariance

It is often difficult to implement a Kalman filter in practical applications due to the inability in obtaining a good estimate of the noise covariance matrix. In our case, we have to estimate the noise covariance of OTS (σ_{ots}) and of IMU (σ_{imu}), which describe the significance of the measured values of OTS and IMU, respectively. As described in Section 3, the measurement accuracy of the OTS varies with the different locations in the workspace. Therefore, σ_{ots} is treated differently in different areas according to the error distribution gained in Section 3:

$$\sigma_{\mathrm{ots}}(x, y, z) = k \cdot \varepsilon(x, y, z), \quad (25)$$

where k is the scale factor and $\varepsilon(x, y, z)$ is the measurement error in a specific area. In contrast, σ_{imu} is treated as a constant due to IMU performance.

6.3 Compensation

As described in Section 1, OTS suffers from the marker-missing problem inevitably caused by disturbance and obstruction from other objects in the workspace. In these cases, OTS may lose its tracking ability or suffer from a severe error. To improve its robustness, compensation is needed when these problems occur. The IMU, which provides continuous reliable data, can make a good compensation to OTS.

During the marker-missing period, the data from OTS cannot be trusted. The noise covariance of OTS is set to infinity so that the Kalman filter takes only the estimated value in the optimization:

$$\sigma_{\mathrm{ots}} \to \infty. \quad (26)$$

We add an ON/OFF value to the Kalman filter. When marker-missing is detected, the Kalman filter will run under the compensation model in which the noise covariance of OTS is set to infinity.

7 Experimental results

Several experiments were performed to verify the proposed method, including drawing a line and a circle with part of OTS data missing, drawing a line and a circle with different speeds using the robot, and finally performing an overall test in the whole workspace of OTS with a dynamic noise covariance due to error distribution. To simplify the data processing, all the experiments were performed in the horizontal plane.

7.1 Compensation

By covering the markers in part of the trajectory when the robot is drawing a line or circle, we want to see the compensation performance.

Fig. 8 shows the result of compensation when drawing a line with a velocity of 500 mm/s. The compensation is still acceptable with about 400 mm of OTS data missing. However, compensation of a line is not very typical. Thus, we also performed the experiment of compensating a circle.

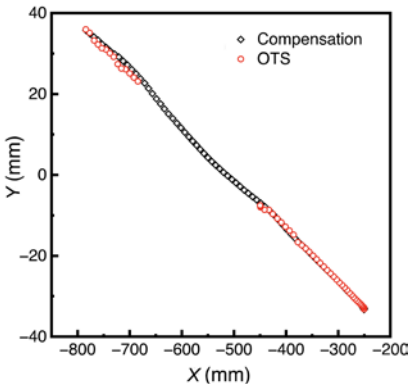

Fig. 8 Compensation of a line

Fig. 9 shows the result of compensation when drawing a circle with a velocity of 2000 mm/s. In such a case, IMU can compensate a distance up to 500 mm.

7.2 Accuracy improvement

The robot shown in Section 4 was used to draw a line and a circle at 500, 1000, and 1500 mm/s, respectively. The performance of the proposed method was evaluated by comparing the tracking results of OTS and data fusion.

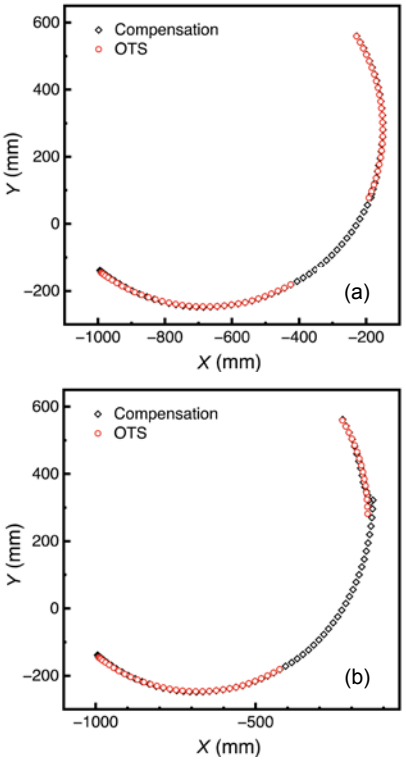

Fig. 9 Compensation of a circle with the compensation distance of 300 mm (a) or 500 mm (b)

Figs. 10a and 11a show the direction and dimension of the acceleration of each position as a vector. With the proposed coordinate frame synchronization method, the acceleration provided by IMU did not show a large error in either direction or dimension, which is a prerequisite to the good result of data fusion. Figs. 10b and 11b show the results from OTS and data fusion. These results were evaluated by data fitting. Tables 1 and 2 show the root mean square error (RMSE) for the line and the circle by OTS and data fusion with different velocities. The performance of OTS was improved using data fusion with an IMU. In the case of drawing a line, an obvious improvement was achieved.

As OTS has an obvious error when drawing a line, a further test was implemented to evaluate the performance of the proposed approach. Several points in the line gained by OTS deviated obviously from the normal direction, while the acceleration data from IMU remained normal (Fig. 12). The deviation was corrected by data fusion.

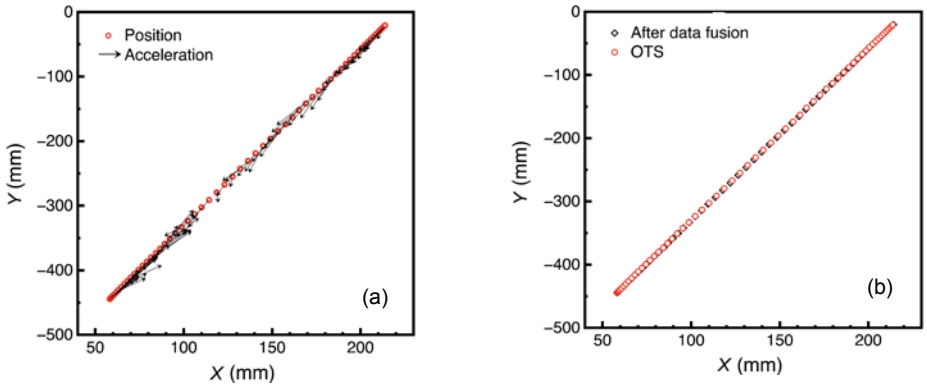

Fig. 10 Results of drawing a line
(a) Position and acceleration; (b) Results before and after data fusion

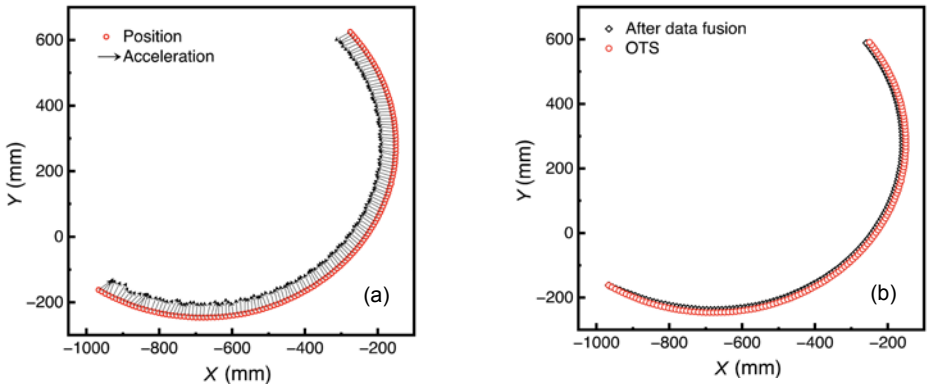

Fig. 11 Results of drawing a circle
(a) Position and acceleration; (b) Results before and after data fusion

Table 1 Accuracy comparison when drawing a line

Velocity (mm/s)	RMSE (mm)	
	OTS	Data fusion
500	0.36	0.24
1000	0.40	0.25

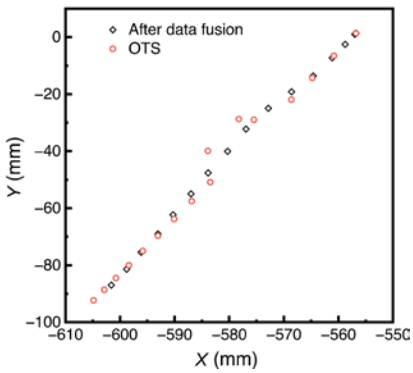

Fig. 12 Data from OTS manually modified to deviate from the normal direction

Table 2 Accuracy comparison when drawing a circle

Velocity (mm/s)	RMSE (mm)	
	OTS	Data fusion
500	0.27	0.26
1000	0.28	0.23
1500	0.36	0.34

7.3 Accuracy improvement in different areas

Based on the error distribution gained in Section 3, the sensors' data of these lines was processed using the Kalman filter with corresponding measurement covariances in different areas.

Fig. 13 shows the total position accuracy improvement of the whole workspace. Fig. 13a shows the error distribution before data fusion. After data fusion, the position error of each area was reduced. Fig. 13b shows the reduced error of different areas, indicating that the accuracy improvements are more obvious in the areas with larger noise covariances.

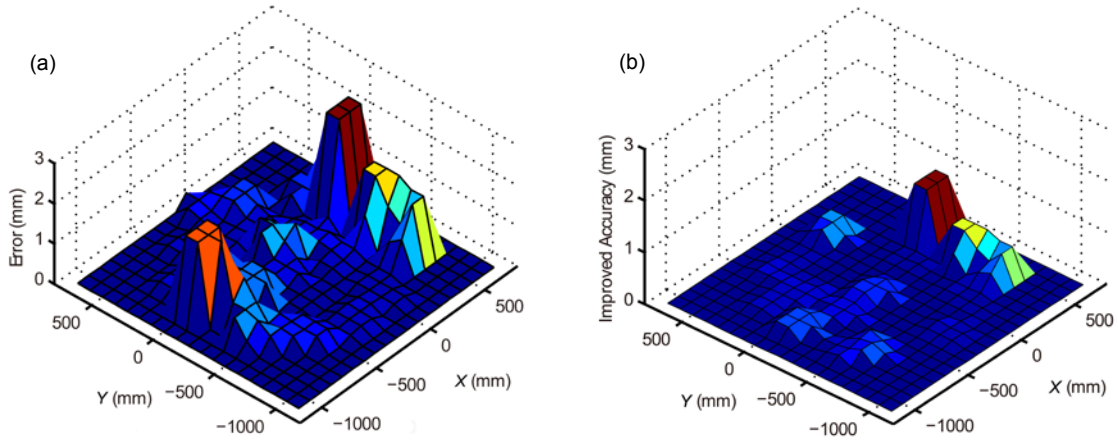

Fig. 13 Position accuracy improvement of OTS
(a) Error distribution before data fusion; (b) Improvement after data fusion

8 Conclusions

A robust optical-inertial data fusion system was proposed for motion tracking of the robot manipulator. Based on the evaluation of error distribution of OTS, a Kalman filter with a dynamic covariance was developed for data fusion. The capability of the developed approach was proved by several experiments, and the performance of OTS was improved in terms of accuracy and reliability.

References

Aristidou, A., Cameron, J., Lasenby, J., 2008. Real-time estimation of missing markers in human motion capture. 2nd Int. Conf. on Bioinformatics and Biomedical Engineering, p.1343-1346. [doi:10.1109/ICBBE.2008.665]

Bleser, G., Stricker, D., 2009. Advanced tracking through efficient image processing and visual–inertial sensor fusion. *Comput. & Graph.*, **33**(1):59-72. [doi:10.1016/j.cag.2008.11.004]

Caron, F., Duflos, E., Pomorski, D., *et al*., 2006. GPS/IMU data fusion using multisensor Kalman filtering: introduction of contextual aspects. *Inform. Fus.*, **7**(2):221-230. [doi:10.1016/j.inffus.2004.07.002]

Claasen, G.C., Martin, P., Picard, F., 2011. Tracking and control for handheld surgery tools. IEEE Biomedical Circuits and Systems Conf., p.428-431. [doi:10.1109/BioCAS.2011.6107819]

Dong, Y., Zwahlen, P., Nguyen, A.M., *et al*., 2010. High performance inertial navigation grade sigma-delta MEMS accelerometer. IEEE/ION Position Location and Navigation Symp., p.32-36. [doi:10.1109/PLANS.2010.5507135]

Foxlin, E., Altshuler, Y., Naimark, L., *et al*., 2004. Flighttracker: a novel optical/inertial tracker for cockpit enhanced vision. Proc. 3rd IEEE/ACM Int. Symp. on Mixed and Augmented Reality, p.212-221. [doi:10.1109/ISMAR.2004.32]

Park, I., Lee, B., Cho, S., *et al*., 2012. Laser-based kinematic calibration of robot manipulator using differential kinematics. *IEEE/ASME Trans. Mechatron.*, **17**(6):1059-1067. [doi:10.1109/TMECH.2011.2158234]

Ren, H., Rank, D., Merdes, M., *et al*., 2012. Multisensor data fusion in an integrated tracking system for endoscopic surgery. *IEEE Trans. Inform. Technol. Biomed.*, **16**(1):106-111. [doi:10.1109/TITB.2011.2164088]

Shirinzadeh, B., Teoh, P., Tian, Y., *et al*., 2010. Laser interferometry-based guidance methodology for high precision positioning of mechanisms and robots. *Robot. Comput.-Integr. Manuf.*, **26**(1):74-82. [doi:10.1016/j.rcim.2009.04.002]

Soroush, A., Farahmand, F., Salarieh, H., 2012. Design and implementation of an improved real-time tracking system for navigation surgery by fusion of optical and inertial tracking methods. *Appl. Mech. Mater.*, **186**:273-279. [doi:10.4028/www.scientific.net/AMM.186.273]

Su, L., Shi, L., Yu, Y., 2009. Collaborative assembly operation between two modular robots based on the optical position feedback. *J. Robot.*, Article ID 214154. [doi:10.1155/2009/214154]

Sukkarieh, S., Nebot, E.M., Durrant-Whyte, H.F., 1999. A high integrity IMU/GPS navigation loop for autonomous land vehicle applications. *IEEE Trans. Robot. Autom.*, **15**(3):572-578. [doi:10.1109/70.768189]

Syed, Z.F., Aggarwal, P., Niu, X., *et al*., 2008. Civilian vehicle navigation: required alignment of the inertial sensors for acceptable navigation accuracies. *IEEE Trans. Veh. Technol.*, **57**(6):3402-3412. [doi:10.1109/TVT.2008.921616]

Tao, Y., Hu, H., 2008. A novel sensing and data fusion system for 3-D arm motion tracking in telerehabilitation. *IEEE*

Trans. Instrum. Meas., **57**(5):1029-1040. [doi:10.1109/TIM.2007.913828]

Wiles, A.D., Thompson, D.G., Frantz, D.D., 2004. Accuracy assessment and interpretation for optical tracking systems. *SPIE*, **5367**:421-432. [doi:10.1117/12.536128]

Xiong, N., Svensson, P., 2002. Multi-sensor management for information fusion: issues and approaches. *Inform. Fus.*, **3**(2):163-186. [doi:10.1016/S1566-2535(02)00055-6]

Yun, X., Calusdian, J., Bachmann, E.R., *et al*., 2012. Estimation of human foot motion during normal walking using inertial and magnetic sensor measurements. *IEEE Trans. Instrum. Meas.*, **61**(7):2059-2072. [doi:10.1109/TIM.2011.2179830]

Zhang, P., Gu, J., Milios, E.E., *et al*., 2005. Navigation with IMU/GPS/digital compass with unscented Kalman filter. IEEE Int. Conf. on Mechatronics and Automation, p.1497-1502. [doi:10.1109/ICMA.2005.1626777]

Zhang, Z.Q., Wu, J.K., 2011. A novel hierarchical information fusion method for three-dimensional upper limb motion estimation. *IEEE Trans. Instrum. Meas.*, **60**(11):3709-3719. [doi:10.1109/TIM.2011.2135070]

Zhou, H., Hu, H., 2010. Reducing drifts in the inertial measurements of wrist and elbow positions. *IEEE Trans. Instrum. Meas.*, **59**(3):575-585. [doi:10.1109/TIM.2009.2025065]